



Observation of $D^0 - \bar{D}^0$ Oscillations

R. Aaij *et al.**

(LHCb Collaboration)

(Received 6 November 2012; published 5 March 2013)

We report a measurement of the time-dependent ratio of $D^0 \rightarrow K^+ \pi^-$ to $D^0 \rightarrow K^- \pi^+$ decay rates in D^{*+} -tagged events using 1.0 fb^{-1} of integrated luminosity recorded by the LHCb experiment. We measure the mixing parameters $x'^2 = (-0.9 \pm 1.3) \times 10^{-4}$, $y' = (7.2 \pm 2.4) \times 10^{-3}$, and the ratio of doubly-Cabibbo-suppressed to Cabibbo-favored decay rates $R_D = (3.52 \pm 0.15) \times 10^{-3}$, where the uncertainties include statistical and systematic sources. The result excludes the no-mixing hypothesis with a probability corresponding to 9.1 standard deviations and represents the first observation of $D^0 - \bar{D}^0$ oscillations from a single measurement.

DOI: [10.1103/PhysRevLett.110.101802](https://doi.org/10.1103/PhysRevLett.110.101802)

PACS numbers: 12.15.Ff, 13.25.Ft, 14.40.Lb

Meson-antimeson oscillations are a manifestation of flavor changing neutral currents that occur because the flavor eigenstates differ from the physical mass eigenstates of the meson-antimeson system. Short-range quark-level transitions as well as long-range processes contribute to this phenomenon. The former are governed by loops in which virtual heavy particles are exchanged, making the study of flavor oscillations an attractive area to search for physics beyond the standard model (SM). Oscillations have been observed in the $K^0 - \bar{K}^0$ [1], $B^0 - \bar{B}^0$ [2], and $B_s^0 - \bar{B}_s^0$ [3] systems, all with rates in agreement with SM expectations. Evidence of $D^0 - \bar{D}^0$ oscillations has been reported by three experiments using different D^0 decay channels [4–8]. Only the combination of these measurements provides confirmation of $D^0 - \bar{D}^0$ oscillations, also referred to as charm mixing, with more than 5σ significance [9]. While it is accepted that charm mixing occurs, a clear observation of the phenomenon from a single measurement is needed to establish it conclusively.

Charm mixing is characterized by two parameters: the mass and decay width differences, Δm and $\Delta\Gamma$, between the two mass eigenstates expressed in terms of the dimensionless quantities $x = \Delta m/\Gamma$ and $y = \Delta\Gamma/2\Gamma$, where Γ is the average D^0 decay width. The charm mixing rate is expected to be small, with predicted values of $|x|, |y| \lesssim \mathcal{O}(10^{-2})$, including significant contributions from nonperturbative long-range processes that compete with the short-range electroweak loops [10–13]. This makes the mixing parameters difficult to calculate and complicates the unambiguous identification of potential non-SM contributions in the experimental measurements [14–16].

In the analysis described in this Letter, $D^0 - \bar{D}^0$ oscillations are observed by studying the time-dependent ratio of $D^0 \rightarrow K^+ \pi^-$ to $D^0 \rightarrow K^- \pi^+$ decay rates [17]. The D^0 flavor at production time is determined using the charge of the soft (low-momentum) pion, π_s^+ , in the strong $D^{*+} \rightarrow D^0 \pi_s^+$ decay. The $D^{*+} \rightarrow D^0(\rightarrow K^- \pi^+) \pi_s^+$ process is referred to as right-sign (RS), whereas the $D^{*+} \rightarrow D^0(\rightarrow K^+ \pi^-) \pi_s^+$ is designated as wrong-sign (WS). The RS process is dominated by a Cabibbo-favored (CF) decay amplitude, whereas the WS amplitude includes contributions from both the doubly-Cabibbo-suppressed (DCS) $D^0 \rightarrow K^+ \pi^-$ decay, as well as $D^0 - \bar{D}^0$ mixing followed by the favored $\bar{D}^0 \rightarrow K^+ \pi^-$ decay. In the limit of small mixing ($|x|, |y| \ll 1$), and assuming negligible CP violation, the time-dependent ratio, R , of WS to RS decay rates is approximated by [10]

$$R(t) \approx R_D + \sqrt{R_D} y' \frac{t}{\tau} + \frac{x'^2 + y'^2}{4} \left(\frac{t}{\tau}\right)^2, \quad (1)$$

where t/τ is the decay time expressed in units of the average D^0 lifetime τ , R_D is the ratio of DCS to CF decay rates, $x' = x \cos \delta + y \sin \delta$, $y' = y \cos \delta - x \sin \delta$, and δ is the strong phase difference between the DCS and CF amplitudes.

The analysis is based on a data sample corresponding to 1.0 fb^{-1} of $\sqrt{s} = 7 \text{ TeV}$ pp collisions recorded by LHCb during 2011. The LHCb detector [18] is a single-arm forward spectrometer covering the pseudorapidity range $2 < \eta < 5$, designed for the study of particles containing b or c quarks. Detector components particularly relevant for this analysis are the silicon Vertex Locator, which provides identification of displaced, secondary vertices of b - and c -hadron decays; the tracking system, which measures charged particles with momentum resolution $\Delta p/p$ that varies from 0.4% at 5 GeV/ c to 0.6% at 100 GeV/ c , corresponding to a typical mass resolution of approximately 8 MeV/ c^2 for a two-body charm-meson decay; and the ring imaging Cherenkov detectors, which provide kaon-pion discrimination.

*Full author list given at the end of the article.

Events are triggered by signatures consistent with a hadronic charm decay. The hardware trigger demands a hadronic energy deposition with a transverse component of at least 3 GeV. Subsequent software-based triggers require two oppositely-charged tracks to form a D^0 candidate with a decay vertex well separated from the associated primary pp collision vertex (PV). Additional requirements on the quality of the online-reconstructed tracks, their transverse momenta (p_T) and their impact parameters (IP), defined as the distance of closest approach of the reconstructed trajectory to the PV, are applied in the final stage of the software trigger. For the offline analysis, only D^0 candidates selected by this trigger algorithm are considered.

The D^0 daughter particles are both required to have $p_T > 800$ MeV/c, $p > 5$ GeV/c, and $\chi^2(\text{IP}) > 9$. The $\chi^2(\text{IP})$ is defined as the difference between the χ^2 of the PV reconstructed with and without the considered particle, and is a measure of consistency with the hypothesis that the particle originates from the PV. Selected D^0 candidates are required to have $p_T > 3.5$ GeV/c and are combined with a track with $p_T > 300$ MeV/c and $p > 1.5$ GeV/c to form a D^{*+} candidate. Contamination from D mesons originating from b -hadron decays (secondary D) is reduced by requiring the $\chi^2(\text{IP})$ of the D^0 and of π_s^+ candidates to be smaller than 9 and 25, respectively. In addition, the ring imaging Cherenkov system is used to distinguish between pions and kaons and to suppress the contamination from misidentified two-body charm decays in the sample. Backgrounds from misidentified singly Cabibbo-suppressed decays are specifically removed by requiring the D^0 candidate mass reconstructed under the K^+K^- and $\pi^+\pi^-$ hypotheses to differ by more than 40 MeV/c² from the known D^0 mass [19]. Contamination from electrons to the soft pion sample is also suppressed using particle identification information. Finally, it is required that the D^0 and the π_s^+ form a vertex,

which is constrained to the measured PV. Only candidates with reconstructed $K\pi$ mass within 24 MeV/c² of the known D^0 mass and with reconstructed $D^0\pi_s^+$ mass below 2.02 GeV/c² are considered further. The $D^0\pi_s^+$ mass, $M(D^0\pi_s^+)$, is calculated using the vector sum of the momenta of the three charged particles and the known D^0 and π^+ masses [19]; no mass hypotheses for the D^0 daughters enter the calculation, ensuring that all two-body signal decays have the same $M(D^0\pi_s^+)$ distribution [20]. Events with multiple RS or WS D^{*+} candidates occur about 2.5% of the time, and all candidates are kept.

Figure 1 shows the $M(D^0\pi_s^+)$ distribution for the selected RS and WS candidates. Overlaid is the result of a binned χ^2 fit used to separate the D^{*+} signal component, with a mass resolution of about 0.3 MeV/c², from the background component, which is dominated by associations of real D^0 decays and random pions. The signal mass shape is modeled as the sum of one Johnson S_U [21] and three Gaussian distributions, which account for the asymmetric tails and the central core of the distribution, respectively. The background is described by an empirical function of the form $[M(D^0\pi_s^+) - m_0]^a e^{-b[M(D^0\pi_s^+) - m_0]}$, where the threshold m_0 is fixed to the sum of the known D^0 and π^+ masses [19]. We reconstruct approximately 3.6×10^4 WS and 8.4×10^6 RS decays. To determine the time-dependent WS/RS ratio, the data are divided into thirteen D^0 decay time bins, chosen to have a similar number of candidates in each bin. The decay time is estimated from the distance L between the PV and the D^0 decay vertex and from the D^0 momentum as $t/\tau = m_{D^0}L/p\tau$, where m_{D^0} and τ are the known D^0 mass and lifetime [19], respectively. The typical decay-time resolution is $\sim 0.1\tau$. The signal yields for the RS and WS samples are determined in each decay time bin using fits to the $M(D^0\pi_s^+)$ distribution. The shape parameters and the

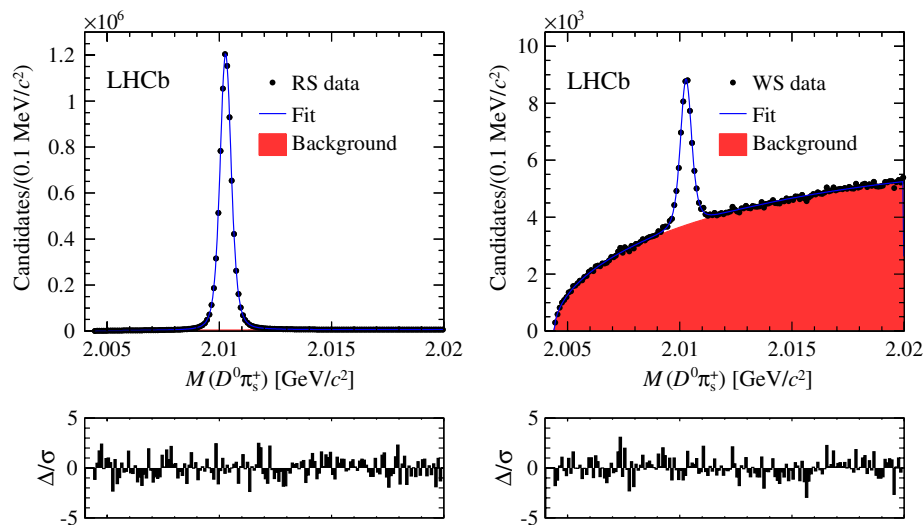


FIG. 1 (color online). Time-integrated $D^0\pi_s^+$ mass distributions for the selected RS $D^0 \rightarrow K^- \pi^+$ (left) and WS $D^0 \rightarrow K^+ \pi^-$ (right) candidates with fit projections overlaid. The bottom plots show the normalized residuals between the data points and the fits.

yields of the two components, signal and random pion background, are left free to vary in the different decay time bins. We further assume that the $M(D^0\pi_s^+)$ signal shape for RS and WS decays are the same. Hence, we first perform a fit to the abundant and cleaner RS sample to determine the signal shape and yield, and then, use those shape parameters with fixed values when fitting for the WS signal yield. The signal yields from the thirteen bins are used to calculate the WS/RS ratios, shown in Fig. 2, and the mixing parameters are determined in a binned χ^2 fit to the time-dependence according to Eq. (1).

Since WS and RS events are expected to have the same decay-time acceptance and $M(D^0\pi_s^+)$ distributions, most systematic uncertainties affecting the determination of the signal yields as a function of decay time cancel in the ratio between WS and RS events. Residual biases from noncanceling instrumental and production effects, such as asymmetries in detection efficiencies or in production, are found to modify the WS/RS ratio only by a relative fraction of $\mathcal{O}(10^{-4})$ and are neglected. Uncertainties in the distance between Vertex Locator sensors can lead to a bias of the decay-time scale. The effect has been estimated to be less than 0.1% of the measured time [22] and translates into relative systematic biases of 0.1% and 0.2% on y' and x'^2 , respectively. At the current level of statistical precision, such small effects are negligible.

The main sources of systematic uncertainty are those which could alter the observed decay-time dependence of the WS/RS ratio. Two such sources have been identified: (1) secondary D mesons and (2) backgrounds from charm decays reconstructed with the wrong particle identification assignments, which peak in $M(D^0\pi_s^+)$ and are not accounted for in our mass fit. These effects, discussed below, are expected to depend on the true value of the mixing parameters and are accounted for in the time-dependent fit.

The contamination of charm mesons produced in b -hadron decays could bias the time-dependent measurement, as the reconstructed decay time is calculated with respect to the PV, which, in this case, does not coincide with the D^0 production vertex. When this secondary component is not subtracted, the measured WS/RS ratio can be written as $R(t)[1 - \Delta_B(t)]$, where $R(t)$ is the ratio of promptly-produced candidates according to Eq. (1) and $\Delta_B(t)$ is a time-dependent bias due to the secondary contamination. Since $R(t)$ is measured to be monotonically nondecreasing [9] and the reconstructed decay time for secondary decays overestimates the true decay time of the D^0 meson, it is possible to bound $\Delta_B(t)$, for all decay times, as

$$0 \leq \Delta_B(t) \leq f_B^{\text{RS}}(t) \left[1 - \frac{R_D}{R(t)} \right], \quad (2)$$

where $f_B^{\text{RS}}(t)$ is the fraction of secondary decays in the RS sample at decay time t . The lower bound in Eq. (2)

corresponds to the case when the parent b -hadron decays instantaneously and the reconstructed D^0 decay time is the true decay time. The upper bound corresponds to the case when the D^0 decays instantaneously and the reconstructed decay time t is entirely due to the b -hadron lifetime. Since $\Delta_B \geq 0$, it follows that the background from secondary D decays decreases the observable mixing effect. To include the corresponding systematic uncertainty, we modify the fitting function for the mixing hypothesis assuming the largest possible bias from Eq. (2). The value of $f_B^{\text{RS}}(t)$ is constrained to the measured value, obtained by fitting the $\chi^2(\text{IP})$ distribution of the RS D^0 candidates in bins of decay time. In this fit, the promptly-produced component is described by a time-independent $\chi^2(\text{IP})$ shape, which is derived from data using the candidates with $t < 0.8\tau$. The $\chi^2(\text{IP})$ shape of the secondary component, and its dependence on decay time, is also determined from data by studying the subsample of candidates that are reconstructed, in combination with other tracks in the events, as $B \rightarrow D^*(3)\pi$, $B \rightarrow D^*\mu X$, or $B \rightarrow D^0\mu X$. The measured value of $f_B^{\text{RS}}(t)$ increases almost linearly with decay time from $(0.0 \pm 0.5)\%$ up to $(14 \pm 5)\%$, for a time-integrated value of $(2.7 \pm 0.2)\%$. We checked on pseudoexperiments, before fitting the data, and then also on data that such a small contamination results in a shift on the measured mixing parameters that is much smaller than the increase in the uncertainty when the secondary bias is included in the fit.

Background from incorrectly reconstructed D meson decays, peaking in the $M(D^0\pi_s^+)$ distribution, arises from D^{*+} decays for which the correct soft pion is found but the D^0 is partially reconstructed or misidentified. This background is suppressed by the use of tight particle identification and two-body mass requirements. From studies of the events in the D^0 mass sidebands, we find that the dominant peaking background is from RS events that survive the requirements of the WS selection; they are estimated to constitute $(0.4 \pm 0.2)\%$ of the WS signal. This contamination is expected to have the same decay time dependence of RS decays and, if neglected, would lead to a small increase in the measured value of R_D . From the events in the D^0 mass sidebands, we derive a bound on the possible time dependence of this background, which is included in the fit in a similar manner to the secondary background. Contamination from peaking background due to partially reconstructed D^0 decays is found to be much smaller than 0.1% of the WS signal and neglected in the fit.

The χ^2 that is minimized in the fit to the WS/RS decay-time dependence is

$$\chi^2(r_i, t_i, \sigma_i | \boldsymbol{\theta}) = \sum_i \left(\frac{r_i - R(t_i | \boldsymbol{\theta}) [1 - \Delta_B(t_i | \boldsymbol{\theta})] - \Delta_p(t_i | \boldsymbol{\theta})}{\sigma_i} \right)^2 + \chi_B^2(\boldsymbol{\theta}) + \chi_p^2(\boldsymbol{\theta}), \quad (3)$$

where r_i and σ_i are the measured WS/RS ratio and its statistical uncertainty in the decay time bin i , respectively.

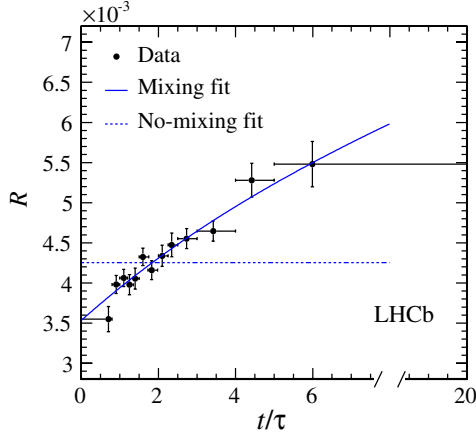


FIG. 2 (color online). Decay-time evolution of the ratio, R , of WS $D^0 \rightarrow K^+ \pi^-$ to RS $D^0 \rightarrow K^- \pi^+$ yields (points) with the projection of the mixing allowed (solid line) and no-mixing (dashed line) fits overlaid.

The decay time, t_i , is the average value in each bin of the RS sample. The fit parameters, θ , include the three mixing parameters (R_D , y' , x'^2) and five nuisance parameters used to describe the decay time evolution of the secondary D fraction (Δ_B) and of the peaking background (Δ_p). The nuisance parameters are constrained to the measured values by the additional χ_B^2 and χ_p^2 terms, which account for their uncertainties including correlations.

The analysis procedure is defined prior to fitting the data for the mixing parameters. Measurements on pseudoexperiments that mimic the experimental conditions of the data, and where $D^0 - \bar{D}^0$ oscillations are simulated, indicate that the fit procedure is stable and free of any bias.

The fit to the decay-time evolution of the WS/RS ratio is shown in Fig. 2 (solid line), with the values and uncertainties of the parameters R_D , y' and x'^2 listed in Table I. The value of x'^2 is found to be negative but consistent with zero. As the dominant systematic uncertainties are treated within the fit procedure (all other systematic effects are negligible), the quoted errors account for systematic as well as statistical uncertainties. When the systematic biases are not included in the fit, the estimated uncertainties on R_D , y' , and x'^2 become, respectively 6%, 10%, and 11% smaller,

TABLE I. Results of the time-dependent fit to the data. The uncertainties include statistical and systematic sources; ndf indicates the number of degrees of freedom.

Fit type (χ^2/ndf)	Parameter	Fit result (10^{-3})	Correlation coefficient		
			R_D	y'	x'^2
Mixing (9.5/10)	R_D	3.52 ± 0.15	1	-0.954	+0.882
	y'	7.2 ± 2.4		1	-0.973
	x'^2	-0.09 ± 0.13			1
No mixing (98.1/12)	R_D	4.25 ± 0.04			

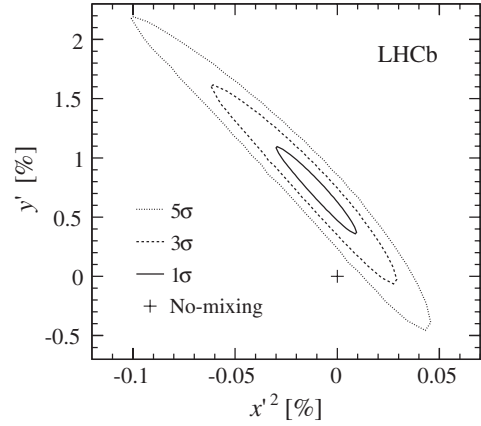


FIG. 3. Estimated confidence-level (C.L.) regions in the (x'^2, y') plane for $1 - \text{C.L.} = 0.317$ (1σ), 2.7×10^{-3} (3σ), and 5.73×10^{-7} (5σ). Systematic uncertainties are included. The cross indicates the no-mixing point.

showing that the quoted uncertainties are dominated by their statistical component. To evaluate the significance of this mixing result, we determine the change in the fit χ^2 when the data are described under the assumption of the no-mixing hypothesis (dashed line in Fig. 2). Under the assumption that the χ^2 difference, $\Delta\chi^2$, follows a χ^2 distribution for two degrees of freedom, $\Delta\chi^2 = 88.6$ corresponds to a p -value of 5.7×10^{-20} , which excludes the no-mixing hypothesis at 9.1 standard deviations. This is illustrated in Fig. 3 where the 1σ , 3σ , and 5σ confidence regions for x'^2 and y' are shown.

As additional cross-checks, we perform the measurement in statistically independent subsamples of the data, selected according to different data-taking periods, and find compatible results. We also use alternative decay-time binning schemes, selection criteria or fit methods to separate signal and background, and find no significant variations in the estimated parameters. Finally, to assess the impact of events where more than one candidate is reconstructed, we repeat the time-dependent fit on data after randomly removing the additional candidates and selecting only one per event; the change in the measured value of R_D , y' , and x'^2 is 2%, 6%, and 7% of their uncertainty, respectively.

In conclusion, we measure the decay time dependence of the ratio between $D^0 \rightarrow K^+ \pi^-$ and $D^0 \rightarrow K^- \pi^+$ decays using 1.0 fb^{-1} of data and exclude the no-mixing hypothesis at 9.1 standard deviations. This is the first observation of $D^0 - \bar{D}^0$ oscillations in a single measurement. The measured values of the mixing parameters are compatible with and have substantially better precision than those from previous measurements [4,6,23].

We express our gratitude to our colleagues in the CERN accelerator departments for the excellent performance of the LHC. We thank the technical and administrative staff at the LHCb institutes. We acknowledge support from CERN and from the national agencies: CAPES, CNPq, FAPERJ,

and FINEP (Brazil); NSFC (China); CNRS/IN2P3 and Region Auvergne (France); BMBF, DFG, HGF, and MPG (Germany); SFI (Ireland); INFN (Italy); FOM and NWO (The Netherlands); SCSR (Poland); ANCS/IFA (Romania); MinES, Rosatom, RFBR, and NRC “Kurchatov Institute” (Russia); MinECo, XuntaGal, and GENCAT (Spain); SNSF and SER (Switzerland); NAS Ukraine (Ukraine); STFC (United Kingdom); NSF (USA). We also acknowledge the support received from the ERC under FP7. The Tier1 computing centres are supported by IN2P3 (France), KIT and BMBF (Germany), INFN (Italy), NWO and SURF (The Netherlands), PIC (Spain), and GridPP (United Kingdom). We are thankful for the computing resources put at our disposal by Yandex LLC (Russia) as well as to the communities behind the multiple open source software packages that we depend on.

-
- [1] K. Lande, E. Booth, J. Impeduglia, L. Lederman, and W. Chinowsky, *Phys. Rev.* **103**, 1901 (1956).
- [2] H. Albrecht *et al.* (ARGUS collaboration), *Phys. Lett. B* **192**, 245 (1987).
- [3] A. Abulencia *et al.* (CDF collaboration), *Phys. Rev. Lett.* **97**, 242003 (2006).
- [4] B. Aubert *et al.* (BABAR collaboration), *Phys. Rev. Lett.* **98**, 211802 (2007).
- [5] M. Staric *et al.* (Belle collaboration), *Phys. Rev. Lett.* **98**, 211803 (2007).
- [6] T. Aaltonen *et al.* (CDF collaboration), *Phys. Rev. Lett.* **100**, 121802 (2008).
- [7] B. Aubert *et al.* (BABAR collaboration), *Phys. Rev. Lett.* **103**, 211801 (2009).
- [8] B. Aubert *et al.* (BABAR collaboration), *Phys. Rev. D* **80**, 071103 (2009).
- [9] Y. Amhis *et al.* (Heavy Flavor Averaging Group), [arXiv:1207.1158](https://arxiv.org/abs/1207.1158).
- [10] S. Bianco, F. Fabbri, D. Benson, and I. Bigi, *Riv. Nuovo Cimento* **26N7**, 1 (2003).
- [11] G. Burdman and I. Shipsey, *Annu. Rev. Nucl. Part. Sci.* **53**, 431 (2003).
- [12] I. Shipsey, *Int. J. Mod. Phys. A* **21**, 5381 (2006).
- [13] M. Artuso, B. Meadows, and A. A. Petrov, *Annu. Rev. Nucl. Part. Sci.* **58**, 249 (2008).
- [14] A. A. Petrov, *Int. J. Mod. Phys. A* **21**, 5686 (2006).
- [15] E. Golowich, J. Hewett, S. Pakvasa, and A. A. Petrov, *Phys. Rev. D* **76**, 095009 (2007).
- [16] M. Ciuchini, E. Franco, D. Guadagnoli, V. Lubicz, M. Pierini, V. Porretti, and L. Silvestrini, *Phys. Lett. B* **655**, 162 (2007).
- [17] The inclusion of charge-conjugated modes is implied throughout this Letter.
- [18] A. A. Alves, Jr. *et al.* (LHCb collaboration), *JINST* **3**, S08005 (2008).
- [19] J. Beringer *et al.* (Particle Data Group), *Phys. Rev. D* **86**, 010001 (2012).
- [20] T. Aaltonen *et al.* (CDF collaboration), *Phys. Rev. D* **85**, 012009 (2012).
- [21] N. L. Johnson, *Biometrika* **36**, 149 (1949).
- [22] R. Aaij *et al.* (LHCb collaboration), *Phys. Lett. B* **716**, 393 (2012).
- [23] L. Zhang *et al.* (Belle collaboration), *Phys. Rev. Lett.* **96**, 151801 (2006).
-
- R. Aaij,³⁸ C. Abellan Beteta,^{33,n} A. Adametz,¹¹ B. Adeva,³⁴ M. Adinolfi,⁴³ C. Adrover,⁶ A. Affolder,⁴⁹ Z. Ajaltouni,⁵ J. Albrecht,³⁵ F. Alessio,³⁵ M. Alexander,⁴⁸ S. Ali,³⁸ G. Alkhazov,²⁷ P. Alvarez Cartelle,³⁴ A. A. Alves Jr,²² S. Amato,² Y. Amhis,³⁶ L. Anderlini,^{17,f} J. Anderson,³⁷ R. Andreassen,⁵⁷ R. B. Appleby,⁵¹ O. Aquines Gutierrez,¹⁰ F. Archilli,^{18,35} A. Artamonov,³² M. Artuso,⁵³ E. Aslanides,⁶ G. Auremma,^{22,m} S. Bachmann,¹¹ J. J. Back,⁴⁵ C. Baesso,⁵⁴ W. Baldini,¹⁶ R. J. Barlow,⁵¹ C. Barschel,³⁵ S. Barsuk,⁷ W. Barter,⁴⁴ A. Bates,⁴⁸ Th. Bauer,³⁸ A. Bay,³⁶ J. Beddow,⁴⁸ I. Bediaga,¹ S. Belogurov,²⁸ K. Belous,³² I. Belyaev,²⁸ E. Ben-Haim,⁸ M. Benayoun,⁸ G. Bencivenni,¹⁸ S. Benson,⁴⁷ J. Benton,⁴³ A. Berezhnoy,²⁹ R. Bernet,³⁷ M.-O. Bettler,⁴⁴ M. van Beuzekom,³⁸ A. Bien,¹¹ S. Bifani,¹² T. Bird,⁵¹ A. Bizzeti,^{17,h} P. M. Bjørnstad,⁵¹ T. Blake,³⁵ F. Blanc,³⁶ C. Blanks,⁵⁰ J. Blouw,¹¹ S. Blusk,⁵³ A. Bobrov,³¹ V. Bocci,²² A. Bondar,³¹ N. Bondar,²⁷ W. Bonivento,¹⁵ S. Borghi,^{51,48} A. Borgia,⁵³ T. J. V. Bowcock,⁴⁹ E. Bowen,³⁷ C. Bozzi,¹⁶ T. Brambach,⁹ J. van den Brand,³⁹ J. Bressieux,³⁶ D. Brett,⁵¹ M. Britsch,¹⁰ T. Britton,⁵³ N. H. Brook,⁴³ H. Brown,⁴⁹ A. Büchler-Germann,³⁷ I. Burducea,²⁶ A. Bursche,³⁷ J. Buytaert,³⁵ S. Cadeddu,¹⁵ O. Callot,⁷ M. Calvi,^{20,j} M. Calvo Gomez,^{33,n} A. Camboni,³³ P. Campana,^{18,35} A. Carbone,^{14,c} G. Carboni,^{21,k} R. Cardinale,^{19,i} A. Cardini,¹⁵ H. Carranza-Mejia,⁴⁷ L. Carson,⁵⁰ K. Carvalho Akiba,² G. Casse,⁴⁹ M. Cattaneo,³⁵ Ch. Cauet,⁹ M. Charles,⁵² Ph. Charpentier,³⁵ P. Chen,^{3,36} N. Chiapolini,³⁷ M. Chrzaszcz,²³ K. Ciba,³⁵ X. Cid Vidal,³⁴ G. Ciezarek,⁵⁰ P. E. L. Clarke,⁴⁷ M. Clemencic,³⁵ H. V. Cliff,⁴⁴ J. Closier,³⁵ C. Coca,²⁶ V. Coco,³⁸ J. Cogan,⁶ E. Cogneras,⁵ P. Collins,³⁵ A. Comerma-Montells,³³ A. Contu,^{15,52} A. Cook,⁴³ M. Coombes,⁴³ G. Corti,³⁵ B. Couturier,³⁵ G. A. Cowan,³⁶ D. Craik,⁴⁵ S. Cunliffe,⁵⁰ R. Currie,⁴⁷ C. D’Ambrosio,³⁵ P. David,⁸ P. N. Y. David,³⁸ I. De Bonis,⁴ K. De Bruyn,³⁸ S. De Capua,⁵¹ M. De Cian,³⁷ J. M. De Miranda,¹ L. De Paula,² P. De Simone,¹⁸ D. Decamp,⁴ M. Deckenhoff,⁹ H. Degaudenzi,^{36,35} L. Del Buono,⁸ C. Deplano,¹⁵ D. Derkach,¹⁴ O. Deschamps,⁵ F. Dettori,³⁹ A. Di Canto,¹¹ J. Dickens,⁴⁴ H. Dijkstra,³⁵ P. Diniz Batista,¹ M. Dogaru,²⁶ F. Domingo Bonal,^{33,n} S. Donleavy,⁴⁹ F. Dordei,¹¹ A. Dosil Suárez,³⁴ D. Dossett,⁴⁵ A. Dovbnya,⁴⁰ F. Dupertuis,³⁶ R. Dzhelyadin,³² A. Dziurda,²³ A. Dzyuba,²⁷ S. Easo,^{46,35} U. Egede,⁵⁰ V. Egorychev,²⁸ S. Eidelman,³¹ D. van Eijk,³⁸ S. Eisenhardt,⁴⁷

R. Ekelhof,⁹ L. Eklund,⁴⁸ I. El Rifai,⁵ Ch. Elsasser,³⁷ D. Elsby,⁴² A. Falabella,^{14,e} C. Färber,¹¹ G. Fardell,⁴⁷ C. Farinelli,³⁸ S. Farry,¹² V. Fave,³⁶ V. Fernandez Albor,³⁴ F. Ferreira Rodrigues,¹ M. Ferro-Luzzi,³⁵ S. Filippov,³⁰ C. Fitzpatrick,³⁵ M. Fontana,¹⁰ F. Fontanelli,^{19,i} R. Forty,³⁵ O. Francisco,² M. Frank,³⁵ C. Frei,³⁵ M. Frosini,^{17,f} S. Furcas,²⁰ A. Gallas Torreira,³⁴ D. Galli,^{14,c} M. Gandelman,² P. Gandini,⁵² Y. Gao,³ J. Garofoli,⁵³ P. Garosi,⁵¹ J. Garra Tico,⁴⁴ L. Garrido,³³ C. Gaspar,³⁵ R. Gauld,⁵² E. Gersabeck,¹¹ M. Gersabeck,⁵¹ T. Gershon,^{45,35} Ph. Ghez,⁴ V. Gibson,⁴⁴ V. V. Gligorov,³⁵ C. Göbel,⁵⁴ D. Golubkov,²⁸ A. Golutvin,^{50,28,35} A. Gomes,² H. Gordon,⁵² M. Grabalosa Gándara,³³ R. Graciani Diaz,³³ L. A. Granado Cardoso,³⁵ E. Graugés,³³ G. Graziani,¹⁷ A. Grecu,²⁶ E. Greening,⁵² S. Gregson,⁴⁴ O. Grünberg,⁵⁵ B. Gui,⁵³ E. Gushchin,³⁰ Yu. Guz,³² T. Gys,³⁵ C. Hadjivasiliou,⁵³ G. Haefeli,³⁶ C. Haen,³⁵ S. C. Haines,⁴⁴ S. Hall,⁵⁰ T. Hampson,⁴³ S. Hansmann-Menzemer,¹¹ N. Harnew,⁵² S. T. Harnew,⁴³ J. Harrison,⁵¹ P. F. Harrison,⁴⁵ T. Hartmann,⁵⁵ J. He,⁷ V. Heijne,³⁸ K. Hennessy,⁴⁹ P. Henrard,⁵ J. A. Hernando Morata,³⁴ E. van Herwijnen,³⁵ E. Hicks,⁴⁹ D. Hill,⁵² M. Hoballah,⁵ C. Hombach,⁵¹ P. Hopchev,⁴ W. Hulsbergen,³⁸ P. Hunt,⁵² T. Huse,⁴⁹ N. Hussain,⁵² D. Hutchcroft,⁴⁹ D. Hynds,⁴⁸ V. Iakovenko,⁴¹ P. Ilten,¹² J. Imong,⁴³ R. Jacobsson,³⁵ A. Jaeger,¹¹ E. Jans,³⁸ F. Jansen,³⁸ P. Jatou,³⁶ F. Jing,³ M. John,⁵² D. Johnson,⁵² C. R. Jones,⁴⁴ B. Jost,³⁵ M. Kabbalo,⁹ S. Kandybei,⁴⁰ M. Karacson,³⁵ T. M. Karbach,³⁵ I. R. Kenyon,⁴² U. Kerzel,³⁵ T. Ketel,³⁹ A. Keune,³⁶ B. Khanji,²⁰ O. Kochebina,⁷ V. Komarov,^{36,29} R. F. Koopman,³⁹ P. Koppenburg,³⁸ M. Korolev,²⁹ A. Kozlinskiy,³⁸ L. Kravchuk,³⁰ K. Kreplin,¹¹ M. Kreps,⁴⁵ G. Krocker,¹¹ P. Krokovny,³¹ F. Kruse,⁹ M. Kucharczyk,^{20,23,j} V. Kudryavtsev,³¹ T. Kvaratskheliya,^{28,35} V. N. La Thi,³⁶ D. Lacarrere,³⁵ G. Lafferty,⁵¹ A. Lai,¹⁵ D. Lambert,⁴⁷ R. W. Lambert,³⁹ E. Lanciotti,³⁵ G. Lanfranchi,^{18,35} C. Langenbruch,³⁵ T. Latham,⁴⁵ C. Lazzeroni,⁴² R. Le Gac,⁶ J. van Leerdam,³⁸ J.-P. Lees,⁴ R. Lefèvre,⁵ A. Leflat,^{29,35} J. Lefrançois,⁷ O. Leroy,⁶ T. Lesiak,²³ Y. Li,³ L. Li Gioi,⁵ M. Liles,⁴⁹ R. Lindner,³⁵ C. Linn,¹¹ B. Liu,³ G. Liu,³⁵ J. von Loeben,²⁰ J. H. Lopes,² E. Lopez Asamar,³³ N. Lopez-March,³⁶ H. Lu,³ J. Luisier,³⁶ H. Luo,⁴⁷ A. Mac Raighne,⁴⁸ F. Machefert,⁷ I. V. Machikhiliyan,^{4,28} F. Maciuc,²⁶ O. Maev,^{27,35} M. Maino,²⁰ S. Malde,⁵² G. Manca,^{15,d} G. Mancinelli,⁶ N. Mangiafave,⁴⁴ U. Marconi,¹⁴ R. Märki,³⁶ J. Marks,¹¹ G. Martellotti,²² A. Martens,⁸ L. Martin,⁵² A. Martí Sánchez,⁷ M. Martinelli,³⁸ D. Martinez Santos,³⁴ D. Martins Tostes,² A. Massafferri,¹ R. Matev,³⁵ Z. Mathe,³⁵ C. Matteuzzi,²⁰ M. Matveev,²⁷ E. Maurice,⁶ A. Mazurov,^{16,30,35,e} J. McCarthy,⁴² R. McNulty,¹² B. Meadows,⁵⁷ M. Meissner,¹¹ M. Merk,³⁸ D. A. Milanes,¹³ M.-N. Minard,⁴ J. Molina Rodriguez,⁵⁴ S. Monteil,⁵ D. Moran,⁵¹ P. Morawski,²³ R. Mountain,⁵³ I. Mous,³⁸ F. Muheim,⁴⁷ K. Müller,³⁷ R. Muresan,²⁶ B. Muryn,²⁴ B. Muster,³⁶ P. Naik,⁴³ T. Nakada,³⁶ R. Nandakumar,⁴⁶ I. Nasteva,¹ M. Needham,⁴⁷ N. Neufeld,³⁵ A. D. Nguyen,³⁶ T. D. Nguyen,³⁶ C. Nguyen-Mau,^{36,o} M. Nicol,⁷ V. Niess,⁵ N. Nikitin,²⁹ T. Nikodem,¹¹ S. Nisar,⁵⁶ A. Nomerotski,^{52,35} A. Novoselov,³² A. Oblakowska-Mucha,²⁴ V. Obraztsov,³² S. Oggero,³⁸ S. Ogilvy,⁴⁸ O. Okhrimenko,⁴¹ R. Oldeman,^{15,35,d} M. Orlandea,²⁶ J. M. Otalora Goicochea,² P. Owen,⁵⁰ B. K. Pal,⁵³ A. Palano,^{13,b} M. Palutan,¹⁸ J. Panman,³⁵ A. Papanestis,⁴⁶ M. Pappagallo,⁴⁸ C. Parkes,⁵¹ C. J. Parkinson,⁵⁰ G. Passaleva,¹⁷ G. D. Patel,⁴⁹ M. Patel,⁵⁰ G. N. Patrick,⁴⁶ C. Patrignani,^{19,i} C. Pavel-Nicorescu,²⁶ A. Pazos Alvarez,³⁴ A. Pellegrino,³⁸ G. Penso,^{22,l} M. Pepe Altarelli,³⁵ S. Perazzini,^{14,c} D. L. Perego,^{20,j} E. Perez Trigo,³⁴ A. Pérez-Calero Yzquierdo,³³ P. Perret,⁵ M. Perrin-Terrin,⁶ G. Pessina,²⁰ K. Petridis,⁵⁰ A. Petrolini,^{19,i} A. Phan,⁵³ E. Picatoste Olloqui,³³ B. Pietrzyk,⁴ T. Pilarč,⁴⁵ D. Pinci,²² S. Playfer,⁴⁷ M. Plo Casasus,³⁴ F. Polci,⁸ G. Polok,²³ A. Poluektov,^{45,31} E. Polcarpo,² D. Popov,¹⁰ B. Popovici,²⁶ C. Potterat,³³ A. Powell,⁵² J. Prisciandaro,³⁶ V. Pugatch,⁴¹ A. Puig Navarro,³⁶ W. Qian,⁴ J. H. Rademacker,⁴³ B. Rakotomiamanana,³⁶ M. S. Rangel,² I. Raniuk,⁴⁰ N. Rauschmayr,³⁵ G. Raven,³⁹ S. Redford,⁵² M. M. Reid,⁴⁵ A. C. dos Reis,¹ S. Ricciardi,⁴⁶ A. Richards,⁵⁰ K. Rinnert,⁴⁹ V. Rives Molina,³³ D. A. Roa Romero,⁵ P. Robbe,⁷ E. Rodrigues,^{51,48} P. Rodriguez Perez,³⁴ G. J. Rogers,⁴⁴ S. Roiser,³⁵ V. Romanovsky,³² A. Romero Vidal,³⁴ J. Rouvinet,³⁶ T. Ruf,³⁵ H. Ruiz,³³ G. Sabatino,^{22,k} J. J. Saborido Silva,³⁴ N. Sagidova,²⁷ P. Sail,⁴⁸ B. Saitta,^{15,d} C. Salzmann,³⁷ B. Sanmartin Sedes,³⁴ M. Sannino,^{19,i} R. Santacesaria,²² C. Santamarina Rios,³⁴ E. Santovetti,^{21,k} M. Sapunov,⁶ A. Sarti,^{18,l} C. Satriano,^{22,m} A. Satta,²¹ M. Savrie,^{16,e} P. Schaack,⁵⁰ M. Schiller,³⁹ H. Schindler,³⁵ S. Schleich,⁹ M. Schlupp,⁹ M. Schmelling,¹⁰ B. Schmidt,³⁵ O. Schneider,³⁶ A. Schopper,³⁵ M.-H. Schune,⁷ R. Schwemmer,³⁵ B. Sciascia,¹⁸ A. Sciubba,^{18,l} M. Seco,³⁴ A. Semennikov,²⁸ K. Senderowska,²⁴ I. Sepp,⁵⁰ N. Serra,³⁷ J. Serrano,⁶ P. Seyfert,¹¹ M. Shapkin,³² I. Shapoval,^{40,35} P. Shatalov,²⁸ Y. Shcheglov,²⁷ T. Shears,^{49,35} L. Shekhtman,³¹ O. Shevchenko,⁴⁰ V. Shevchenko,²⁸ A. Shires,⁵⁰ R. Silva Coutinho,⁴⁵ T. Skwarnicki,⁵³ N. A. Smith,⁴⁹ E. Smith,^{52,46} M. Smith,⁵¹ K. Sobczak,⁵ M. D. Sokoloff,⁵⁷ F. J. P. Soler,⁴⁸ F. Soomro,^{18,35} D. Souza,⁴³ B. Souza De Paula,² B. Spaan,⁹ A. Sparkes,⁴⁷ P. Spradlin,⁴⁸ F. Stagni,³⁵ S. Stahl,¹¹ O. Steinkamp,³⁷ S. Stoica,²⁶ S. Stone,⁵³ B. Storaci,³⁸ M. Straticiu,²⁶ U. Straumann,³⁷ V. K. Subbiah,³⁵ S. Swientek,⁹ M. Szczekowski,²⁵ P. Szczypka,^{36,35} T. Szumlak,²⁴

S. T’Jampens,⁴ M. Teklishyn,⁷ E. Teodorescu,²⁶ F. Teubert,³⁵ C. Thomas,⁵² E. Thomas,³⁵ J. van Tilburg,¹¹
V. Tisserand,⁴ M. Tobin,³⁷ S. Tolc,³⁹ D. Tonelli,³⁵ S. Topp-Joergensen,⁵² N. Torr,⁵² E. Tournefier,^{4,50} S. Tourneur,³⁶
M. T. Tran,³⁶ M. Tresch,³⁷ A. Tsaregorodtsev,⁶ P. Tsopelas,³⁸ N. Tuning,³⁸ M. Ubada Garcia,³⁵ A. Ukleja,²⁵
D. Urner,⁵¹ U. Uwer,¹¹ V. Vagnoni,¹⁴ G. Valenti,¹⁴ R. Vazquez Gomez,³³ P. Vazquez Regueiro,³⁴ S. Vecchi,¹⁶
J. J. Velthuis,⁴³ M. Veltri,^{17,g} G. Veneziano,³⁶ M. Vesterinen,³⁵ B. Viaud,⁷ D. Vieira,² X. Vilasis-Cardona,^{33,n}
A. Vollhardt,³⁷ D. Volyanskyy,¹⁰ D. Voong,⁴³ A. Vorobyev,²⁷ V. Vorobyev,³¹ C. Voß,⁵⁵ H. Voss,¹⁰ R. Waldi,⁵⁵
R. Wallace,¹² S. Wandernoth,¹¹ J. Wang,⁵³ D. R. Ward,⁴⁴ N. K. Watson,⁴² A. D. Webber,⁵¹ D. Websdale,⁵⁰
M. Whitehead,⁴⁵ J. Wicht,³⁵ D. Wiedner,¹¹ L. Wiggers,³⁸ G. Wilkinson,⁵² M. P. Williams,^{45,46} M. Williams,^{50,p}
F. F. Wilson,⁴⁶ J. Wishahi,⁹ M. Witek,²³ W. Witzeling,³⁵ S. A. Wotton,⁴⁴ S. Wright,⁴⁴ S. Wu,³ K. Wyllie,³⁵ Y. Xie,^{47,35}
F. Xing,⁵² Z. Xing,⁵³ Z. Yang,³ R. Young,⁴⁷ X. Yuan,³ O. Yushchenko,³² M. Zangoli,¹⁴ M. Zavertyaev,^{10,a} F. Zhang,³
L. Zhang,⁵³ W. C. Zhang,¹² Y. Zhang,³ A. Zhelezov,¹¹
L. Zhong,³ and A. Zvyagin³⁵

(LHCb Collaboration)

¹Centro Brasileiro de Pesquisas Físicas (CBPF), Rio de Janeiro, Brazil

²Universidade Federal do Rio de Janeiro (UFRJ), Rio de Janeiro, Brazil

³Center for High Energy Physics, Tsinghua University, Beijing, China

⁴LAPP, Université de Savoie, CNRS/IN2P3, Annecy-Le-Vieux, France

⁵Clermont Université, Université Blaise Pascal, CNRS/IN2P3, LPC, Clermont-Ferrand, France

⁶CPPM, Aix-Marseille Université, CNRS/IN2P3, Marseille, France

⁷LAL, Université Paris-Sud, CNRS/IN2P3, Orsay, France

⁸LPNHE, Université Pierre et Marie Curie, Université Paris Diderot, CNRS/IN2P3, Paris, France

⁹Fakultät Physik, Technische Universität Dortmund, Dortmund, Germany

¹⁰Max-Planck-Institut für Kernphysik (MPIK), Heidelberg, Germany

¹¹Physikalisches Institut, Ruprecht-Karls-Universität Heidelberg, Heidelberg, Germany

¹²School of Physics, University College Dublin, Dublin, Ireland

¹³Sezione INFN di Bari, Bari, Italy

¹⁴Sezione INFN di Bologna, Bologna, Italy

¹⁵Sezione INFN di Cagliari, Cagliari, Italy

¹⁶Sezione INFN di Ferrara, Ferrara, Italy

¹⁷Sezione INFN di Firenze, Firenze, Italy

¹⁸Laboratori Nazionali dell’INFN di Frascati, Frascati, Italy

¹⁹Sezione INFN di Genova, Genova, Italy

²⁰Sezione INFN di Milano Bicocca, Milano, Italy

²¹Sezione INFN di Roma Tor Vergata, Roma, Italy

²²Sezione INFN di Roma La Sapienza, Roma, Italy

²³Henryk Niewodniczanski Institute of Nuclear Physics Polish Academy of Sciences, Kraków, Poland

²⁴AGH University of Science and Technology, Kraków, Poland

²⁵National Center for Nuclear Research (NCBJ), Warsaw, Poland

²⁶Horia Hulubei National Institute of Physics and Nuclear Engineering, Bucharest-Magurele, Romania

²⁷Petersburg Nuclear Physics Institute (PNPI), Gatchina, Russia

²⁸Institute of Theoretical and Experimental Physics (ITEP), Moscow, Russia

²⁹Institute of Nuclear Physics, Moscow State University (SINP MSU), Moscow, Russia

³⁰Institute for Nuclear Research of the Russian Academy of Sciences (INR RAN), Moscow, Russia

³¹Budker Institute of Nuclear Physics (SB RAS) and Novosibirsk State University, Novosibirsk, Russia

³²Institute for High Energy Physics (IHEP), Protvino, Russia

³³Universitat de Barcelona, Barcelona, Spain

³⁴Universidad de Santiago de Compostela, Santiago de Compostela, Spain

³⁵European Organization for Nuclear Research (CERN), Geneva, Switzerland

³⁶Ecole Polytechnique Fédérale de Lausanne (EPFL), Lausanne, Switzerland

³⁷Physik-Institut, Universität Zürich, Zürich, Switzerland

³⁸Nikhef National Institute for Subatomic Physics, Amsterdam, The Netherlands

³⁹Nikhef National Institute for Subatomic Physics and VU University Amsterdam, Amsterdam, The Netherlands

⁴⁰NSC Kharkiv Institute of Physics and Technology (NSC KIPT), Kharkiv, Ukraine

⁴¹Institute for Nuclear Research of the National Academy of Sciences (KINR), Kyiv, Ukraine

⁴²University of Birmingham, Birmingham, United Kingdom

⁴³H.H. Wills Physics Laboratory, University of Bristol, Bristol, United Kingdom

⁴⁴*Cavendish Laboratory, University of Cambridge, Cambridge, United Kingdom*

⁴⁵*Department of Physics, University of Warwick, Coventry, United Kingdom*

⁴⁶*STFC Rutherford Appleton Laboratory, Didcot, United Kingdom*

⁴⁷*School of Physics and Astronomy, University of Edinburgh, Edinburgh, United Kingdom*

⁴⁸*School of Physics and Astronomy, University of Glasgow, Glasgow, United Kingdom*

⁴⁹*Oliver Lodge Laboratory, University of Liverpool, Liverpool, United Kingdom*

⁵⁰*Imperial College London, London, United Kingdom*

⁵¹*School of Physics and Astronomy, University of Manchester, Manchester, United Kingdom*

⁵²*Department of Physics, University of Oxford, Oxford, United Kingdom*

⁵³*Syracuse University, Syracuse, New York, USA*

⁵⁴*Pontifícia Universidade Católica do Rio de Janeiro (PUC-Rio), Rio de Janeiro, Brazil [associated with Universidade Federal do Rio de Janeiro (UFRJ), Rio de Janeiro, Brazil]*

⁵⁵*Institut für Physik, Universität Rostock, Rostock, Germany (associated with Physikalisches Institut, Ruprecht-Karls-Universität Heidelberg, Heidelberg, Germany)*

⁵⁶*Institute of Information Technology, COMSATS, Lahore, Pakistan (associated with Syracuse University, Syracuse, New York, USA)*

⁵⁷*University of Cincinnati, Cincinnati, Ohio, USA (associated with Syracuse University, Syracuse, New York, USA)*

^aAlso at P.N. Lebedev Physical Institute, Russian Academy of Science (LPI RAS), Moscow, Russia

^bAlso at Università di Bari, Bari, Italy.

^cAlso at Università di Bologna, Bologna, Italy.

^dAlso at Università di Cagliari, Cagliari, Italy.

^eAlso at Università di Ferrara, Ferrara, Italy.

^fAlso at Università di Firenze, Firenze, Italy.

^gAlso at Università di Urbino, Urbino, Italy.

^hAlso at Università di Modena e Reggio Emilia, Modena, Italy.

ⁱAlso at Università di Genova, Genova, Italy.

^jAlso at Università di Milano Bicocca, Milano, Italy.

^kAlso at Università di Roma Tor Vergata, Roma, Italy.

^lAlso at Università di Roma La Sapienza, Roma, Italy.

^mAlso at Università della Basilicata, Potenza, Italy.

ⁿAlso at LIFAELS, La Salle, Universitat Ramon Llull, Barcelona, Spain.

^oAlso at Hanoi University of Science, Hanoi, Viet Nam.

^pAlso at Massachusetts Institute of Technology, Cambridge, MA, USA.